



ZIBELINE INTERNATIONAL

ISSN: 1024-1752 (Print)

CODEN: JERDFO

DOI : <http://doi.org/10.26480/jmerd.04.2018.24.30>

CrossMark

FERROFLUID LUBRICATION OF A LONGITUDINALLY ROUGH ROTATING CIRCULAR STEP BEARING

J. V. Adeshara*¹, M. B. Prajapati², G. M. Deheri³, R. M. Patel⁴¹ Research Scholar, Department of Mathematics, H. N. G. University, Patan - 384 265, Gujarat State, India.² Head, Department of Mathematics, H. N. G. University, Patan - 384 265, Gujarat State, India.³ Department of Mathematics, S. P. University, Vallabh Vidyanagar - 388 120, Gujarat State, India.⁴ Department of Mathematics, Gujarat Arts and Science College, Ahmedabad - 380 006 Gujarat State, India.* Corresponding Author Email: rmpatel2711@gmail.com, adesharajatin01@gmail.com, rmpatel2711@gmail.com

This is an open access article distributed under the Creative Commons Attribution License, which permits unrestricted use, distribution, and reproduction in any medium, provided the original work is properly cited

ARTICLE DETAILS

ABSTRACT

Article History:

Received 13 September 2018
Accepted 16 October 2018
Available online 7 November 2018

This investigation tries to examine the effect of magnetic fluid lubrication on the behaviour of a longitudinally rough rotating circular step bearing resorting to the stochastic model of Christensen and Tonder. The magnetic fluid flow model given by Neuringer Rosensweig is used here. The pressure distribution is obtained by solving the Reynolds type equation associated with the bearing system. Then the load carrying capacity is calculated. The graphical results presented here establish that the magnetic fluid lubrication offers significant help to the longitudinal roughness pattern to enhance the performance of the bearing system. This assistance of magnetic fluid became more favorable when the plates rotate in opposite direction.

KEYWORDS

Step bearing, roughness, ferrofluid, rotation, load carrying capacity

NOMENCLATURE

r Radial coordinate

r_o Outer radius

r_i Inner radius

$R = \frac{r}{r_o}$

$k = \frac{r_i}{r_o} = \text{Radii ratio}$

h Lubricant film thickness

\dot{h} Squeeze film velocity

μ_0 permeability of the free space

$\bar{\mu}$ Magnetic susceptibility

μ Absolute viscosity of the lubricant

$\mu^* = \frac{h^3 \mu_0 \bar{\mu}}{\mu h} = \text{Dimensionless magnetization parameter}$

p Lubricant pressure

P Non-dimensional pressure

P_s Dimensionless supply pressure

ρ Density of lubricant

S Non-dimensional rotational inertia

Ω_u Angular velocity of upper plate

Ω_l Angular velocity of lower plate

$\Omega_r = \Omega_u - \Omega_l$

$\Omega_s = \Omega_l / \Omega_u = \text{Rotation ratio}$

w Load carrying capacity

W Dimensionless load carrying capacity

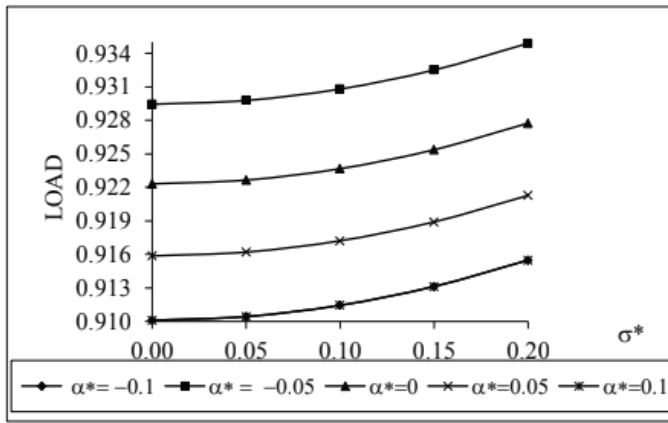


Figure 6: Variation of load carrying capacity with respect to σ^* and α^*

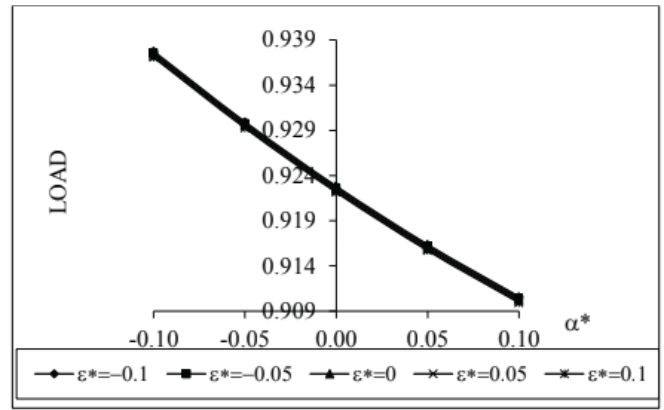


Figure 10: Variation of load carrying capacity with respect to α^* and ϵ^*

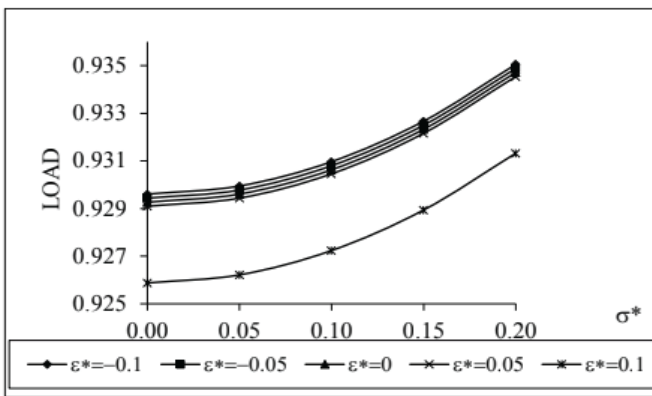


Figure 7: Variation of load carrying capacity with respect to σ^* and ϵ^*

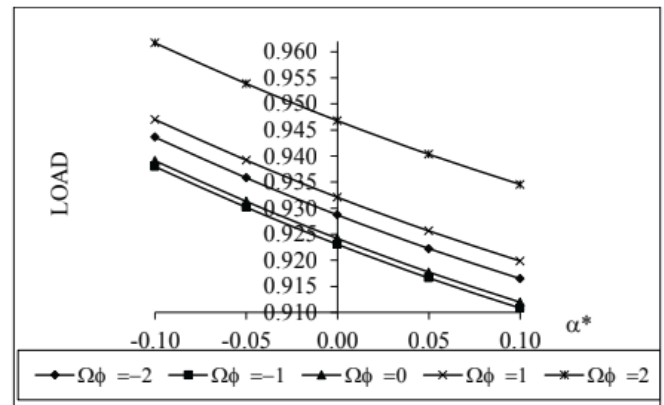


Figure 11: Variation of load carrying capacity with respect to α^* and $\Omega\phi$

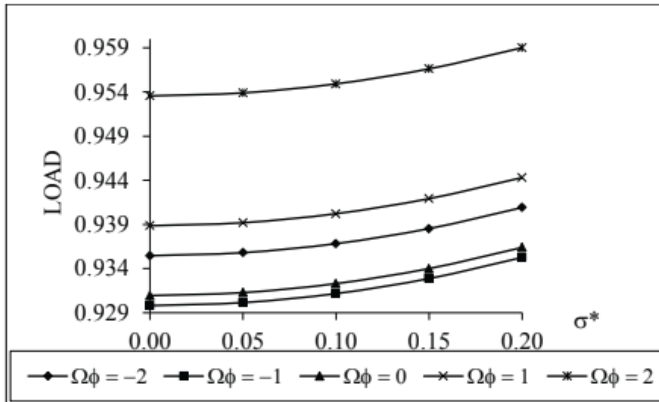


Figure 8: Variation of load carrying capacity with respect to σ^* and $\Omega\phi$

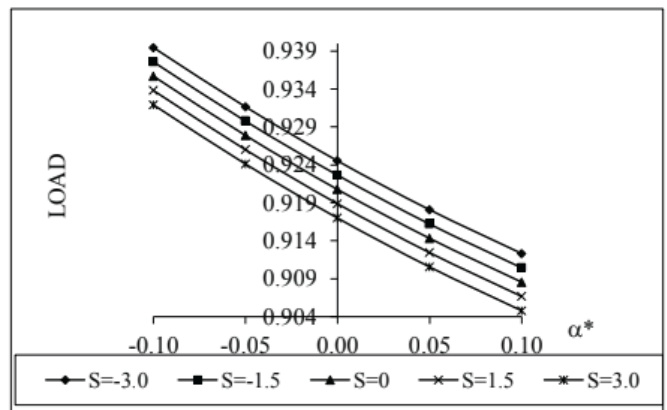


Figure 12: Variation of load carrying capacity with respect to α^* and S

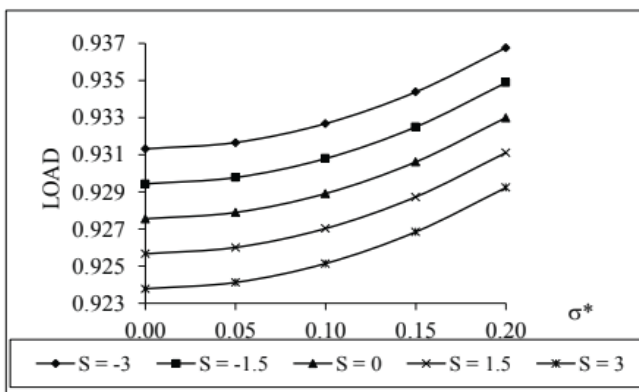


Figure 9: Variation of load carrying capacity with respect to σ^* and S

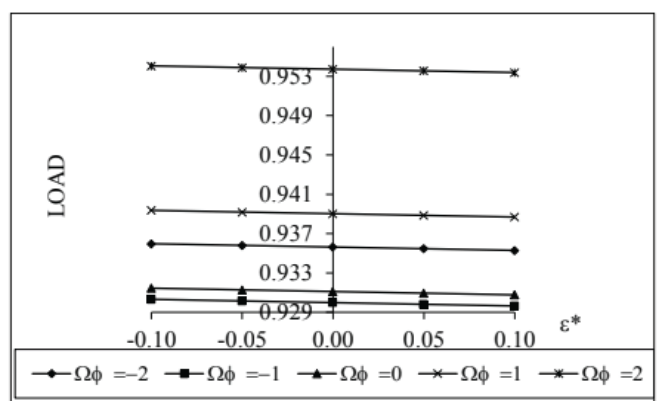


Figure 13: Variation of load carrying capacity with respect to ϵ^* and $\Omega\phi$

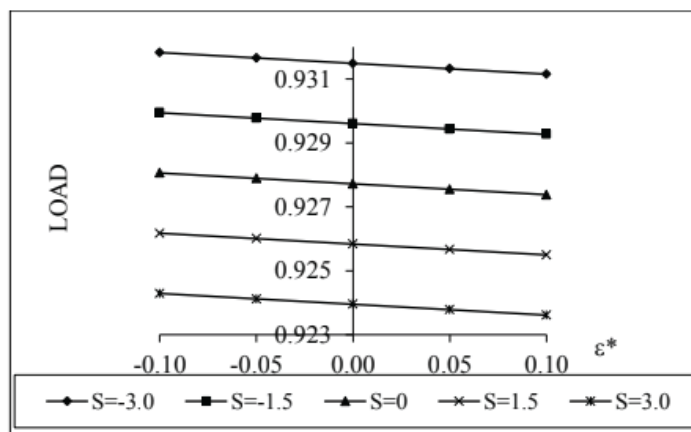


Figure 14: Variation of load carrying capacity with respect to ϵ^* and S

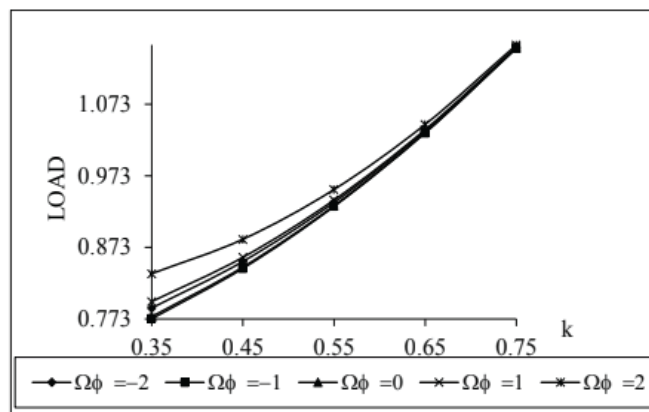


Figure 16: Variation of load carrying capacity with respect to k and $\Omega\phi$

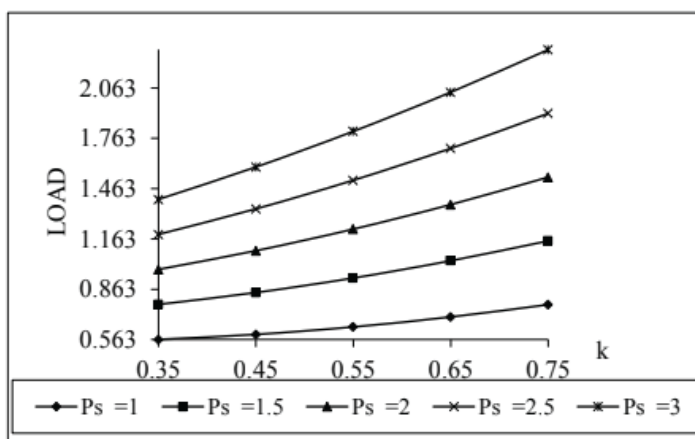


Figure 15: Variation of load carrying capacity with respect to k and P_s

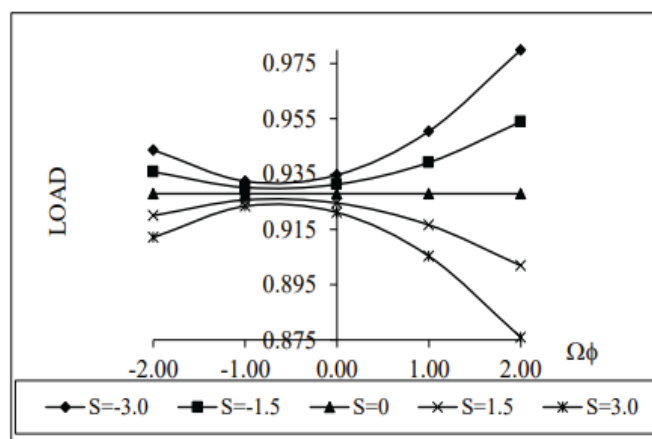


Figure 17: Variation of load carrying capacity with respect to $\Omega\phi$ and S

Table 1: Variation of load carrying capacity for various values of μ^* and k

	$P_s=1$	$P_s=1.5$	$P_s=2$	$P_s=2.5$	$P_s=3$
$\mu^*=0.0000$	0.63357185	0.92524835	1.21692484	1.50860133	1.80027783
$\mu^*=0.0010$	0.63357560	0.92525209	1.21692859	1.50860508	1.80028157
$\mu^*=0.0100$	0.63360932	0.92528581	1.21696231	1.50863880	1.80031529
$\mu^*=0.1000$	0.63394651	0.92562301	1.21729950	1.50897599	1.80065249
$\mu^*=1.0000$	0.63731846	0.92899495	1.22067145	1.51234794	1.80402443

Table 2: Variation of load carrying capacity for various values of μ^* and P_s

	$P_s=1$	$P_s=1.5$	$P_s=2$	$P_s=2.5$	$P_s=3$
$\mu^*=0.0000$	0.63357185	0.92524835	1.21692484	1.50860133	1.80027783
$\mu^*=0.0010$	0.63357560	0.92525209	1.21692859	1.50860508	1.80028157
$\mu^*=0.0100$	0.63360932	0.92528581	1.21696231	1.50863880	1.80031529
$\mu^*=0.1000$	0.63394651	0.92562301	1.21729950	1.50897599	1.80065249
$\mu^*=1.0000$	0.63731846	0.92899495	1.22067145	1.51234794	1.80402443

Table 3: Variation of load carrying capacity for various values of σ^* and k

	k=0.35	k=0.45	k=0.55	k=0.65	k=0.75
$\sigma^* = 0.00$	0.75935967	0.83463388	0.92491164	1.03035116	1.15019558
$\sigma^* = 0.05$	0.76026377	0.83521797	0.92525209	1.03052121	1.15026120
$\sigma^* = 0.10$	0.76297609	0.83697025	0.92627344	1.03103133	1.15045804

$\sigma^* = 0.15$	0.76749660	0.83989071	0.92797569	1.03188154	1.15078610
$\sigma^* = 0.20$	0.77382533	0.84397936	0.93035884	1.03307184	1.15124539

Table 4: Variation of load carrying capacity for various values of σ^* and P_s

	$P_s=1$	$P_s=1.5$	$P_s=2$	$P_s=2.5$	$P_s=3$
$\delta = 0.00$	0.63323515	0.92491164	1.21658814	1.50826463	1.79994112
$\delta = 0.05$	0.63357560	0.92525209	1.21692859	1.50860508	1.80028157
$\delta = 0.10$	0.63459695	0.92627344	1.21794994	1.50962643	1.80130292
$\delta = 0.15$	0.63629920	0.92797569	1.21965219	1.51132868	1.80300517
$\delta = 0.20$	0.63868235	0.93035884	1.22203533	1.51371183	1.80538832

Table 5: Variation of load carrying capacity for various values of δ and k

	$k=0.35$	$k=0.45$	$k=0.55$	$k=0.65$	$k=0.75$
$\alpha^* = 0.10$	0.76898205	0.84085038	0.92853505	1.03216093	1.15089390
$\alpha^* = 0.05$	0.76026377	0.83521797	0.92525209	1.03052121	1.15026120
$\alpha^* = 0.00$	0.75335370	0.83075374	0.92265003	1.02922157	1.14975971
$\alpha^* = 0.05$	0.74824508	0.82745334	0.92072633	1.02826075	1.14938897
$\alpha^* = 0.10$	0.74493116	0.82531239	0.91947844	1.02763747	1.14914847

Table 6: Variation of load carrying capacity for various values of α^* and P_s

	$P_s=1$	$P_s=1.5$	$P_s=2$	$P_s=2.5$	$P_s=3$
$\alpha^* = -0.10$	0.63685856	0.92853505	1.22021155	1.51188804	1.80356453
$\alpha^* = -0.05$	0.63357560	0.92525209	1.21692859	1.50860508	1.80028157
$\alpha^* = 0.00$	0.63097354	0.92265003	1.21432653	1.50600302	1.79767951
$\alpha^* = 0.05$	0.62904984	0.92072633	1.21240282	1.50407932	1.79575581
$\alpha^* = 0.10$	0.62780194	0.91947844	1.21115493	1.50283142	1.79450792

Table 7: Variation of load carrying capacity for various values of ϵ^* and k

	$k=0.35$	$k=0.45$	$k=0.55$	$k=0.65$	$k=0.75$
$\epsilon^* = -0.10$	0.76071414	0.83550892	0.92542168	1.03060591	1.15029388
$\epsilon^* = 0.05$	0.76026377	0.83521797	0.92525209	1.03052121	1.15026120
$\epsilon^* = 0.00$	0.75981341	0.83492701	0.92508250	1.03043650	1.15022851
$\epsilon^* = 0.05$	0.75936305	0.83463606	0.92491292	1.03035180	1.15019583
$\epsilon^* = 0.10$	0.75891268	0.83434510	0.92474333	1.03026709	1.15016314

Table 8: Variation of load carrying capacity for various values of ϵ^* and P_s

	$P_s=1$	$P_s=1.5$	$P_s=2$	$P_s=2.5$	$P_s=3$
$\epsilon^* = -0.10$	0.63374519	0.92542168	1.21709818	1.50877467	1.80045116
$\epsilon^* = -0.05$	0.63357560	0.92525209	1.21692859	1.50860508	1.80028157
$\epsilon^* = 0.00$	0.63340601	0.92508250	1.21675900	1.50843549	1.80011198
$\epsilon^* = 0.05$	0.63323642	0.92491292	1.21658941	1.50826590	1.79994240
$\epsilon^* = 0.10$	0.63306683	0.92474333	1.21641982	1.50809631	1.79977281

Table 10: Variation of load carrying capacity for various values of k and S

	S=-3.0	S=-1.5	S=0	S=1.5	S=3.0
k=0.35	0.76526781	0.76026377	0.75525974	0.75025570	0.74525167
k=0.45	0.83845081	0.83521797	0.83198513	0.82875229	0.82551945
k=0.55	0.92713642	0.92525209	0.92336777	0.92148345	0.91959913
k=0.65	1.03146236	1.03052121	1.02958005	1.02863890	1.02769775
k=0.75	1.15062435	1.15026120	1.14989804	1.14953488	1.14917173

Table 11: Variation of load carrying capacity for various values of Ps and Ω_ϕ

	$\Omega_\phi = -2$	$\Omega_\phi = -1$	$\Omega_\phi = 0$	$\Omega_\phi = 1$	$\Omega_\phi = 2$
Ps=1.00	0.63960543	0.63395246	0.63508306	0.64299721	0.65769492
Ps=1.50	0.93128192	0.92562896	0.92675955	0.93467370	0.94937141
Ps=2.00	1.22295842	1.21730545	1.21843604	1.22635019	1.24104790
Ps=2.50	1.51463491	1.50898194	1.51011254	1.51802669	1.53272440
Ps=3.00	1.80631140	1.80065844	1.80178903	1.80970318	1.82440089

Table 9: Variation of load carrying capacity for various values of Ps and S

	S=-3.0	S=-1.5	S=0	S=1.5	S=3.0
Ps=1.00	0.63545992	0.63357560	0.63169128	0.62980696	0.62792263
Ps=1.50	0.92713642	0.92525209	0.92336777	0.92148345	0.91959913
Ps=2.00	1.21881291	1.21692859	1.21504426	1.21315994	1.21127562
Ps=2.50	1.51048940	1.50860508	1.50672076	1.50483644	1.50295211
Ps=3.00	1.80216590	1.80028157	1.79839725	1.79651293	1.79462861

REFERENCES

[1] Elwell, R., C., Sternlicht, B. 1960. Theoretical and experimental analysis of hydrostatic thrust bearings, Basic Engineering, Transaction of ASME, D, 82, 505- 512.

[2] Dowson, D.1961. Inertia effects in hydrostatic thrust bearing, Journal of basic engineering, Transaction of ASME, D, 83, 227.

[3] Majumdar, B., C., Ghosh, B.1970. Load and flow parameters of externally pressurized oil lubricated rectangular thrust bearings, M. E. Division, The Institutes of Engineering, 50(1), 253-257.

[4] Ghosh, M., K., Majumdar, B., C. 1982. Dynamic stiffness and damping characteristic of compensated hydrostatic thrust bearings, Journal of Lubrication Technology, Transaction of ASME, F, 104, 491-496.

[5] Christensen, H., Tonder, K. C. 1969a. Tribology of rough surface: Stochastic model of hydrodynamic lubrication, SINTEF Report No. 10/69-18.

[6] Christensen, H., Tonder, K. C. 1969b. Tribology of rough surface: Parametric study and comparison of lubrication models, SINTEF Report No. 22/69-18.

[7] Christensen, H., Tonder, K., C. 1970. The hydrodynamic lubrication of rough bearing surface of finite width, ASME-ASLE Lubrication Conference, 70-Lubrication 7.

[8] Ting, L., L. 1975. Engagement behavior of lubricated porous annular disks part I: Squeeze film phase surface roughness and elastic deformation effects, Wear, 34.159-182.

[9] Prakash, J., Tiwari, K. 1983. Roughness effect in porous circular

squeeze plates with arbitrary wall thickness, Journal of Lubrication Technology, 105, 90.

[10] Prajapati, B. L. 1995. On certain theoretical studies in hydrodynamics and electrohydrodynamic lubrication, Dissertation, Ph. D. Thesis, S. P. University, V. V. Nagar.

[11] Andharia, P., I., Gupta, J., L., Deheri, G., M. 1999. Effect of transverse surface roughness on the behavior of squeeze film in a spherical bearing, Proceedings of International Conference: Problem of Non-Conventional Bearing Systems NCBS'99, Journal of Applied Mechanics and Engineering, Special Issue, 4, 19-24.

[12] Naduvinamani, N., B., Kadadi, A., K. 2013. Effect of viscosity variation on the micropolar fluid squeeze film lubrication of a short journal bearing, Advances in Tribology, Article ID 743987, 7 pages, <https://doi.org/10.1155/2013/743>.

[13] Lin, J., R., Chinang, C., F. 2002. Effect of surface roughness and rotational inertia on the optimal stiffness of hydrostatic thrust bearings, International Journal of Applied Mechanics and Engineering, 7(4), 1247-1261.

[14] Patel, R., M., Deheri, G., M. 2003. Magnetic fluid-based squeeze film behaviour between rotating porous circular plates with a concentric circular pocket and surface roughness effects, International Journal of Applied Mechanics and Engineering, 8(2), 271-277.

[15] Deheri, G., M., Patel, H., C., Patel, R., M. 2006. Performance of magnetic fluid based circular step bearing, MECHANIKA, 57(1), 22-27.

[16] Majumdar, B. C.1985. Introduction to Tribology of Bearings, Wheeler Publisher, Wheeler Co. Ltd., India.

[17] Andharia, P., I., Deheri, G., M. 2001. Effect of longitudinal surface roughness on the behaviour of squeeze film in a spherical bearing, *International Journal of Applied Mechanics and Engineering*, 6(4), p.p. 885-897.

[18] Andharia, P., I., Deheri, G., M., 2010, Longitudinal roughness effect on magnetic fluid-based squeeze film between conical, *Industrial Lubrication and Tribology*, 62(5), p.p. 285-291.

[19] Andharia, P., I., Deheri, G. M. 2013. Performance of magnetic fluid-based squeeze film between longitudinally rough elliptical plates, *ISRN Tribology*, Article ID482604, 6.

[20] Shimpi, M., E., Deheri, G., M. 2016. Combine effect of bearing deformation and longitudinal roughness on the performance of a ferrofluid based squeeze film together with velocity slip in truncated conical plates, *Imperial journal of Interdisciplinary research*, 2(8), p.p. 1423-1430.

[21] Adeshara, J., V., Prajapati, M., B., Deheri, G., M., Patel, R., M. 2018. A Study of Hydromagnetic Longitudinal Rough Circular Step Bearing, *Advances in Tribology*, Article ID 3981087, 7 pages, <https://doi.org/10.1155/2018/3981087>.

[22] Lin, J. R. 2016. Longitudinal surface roughness effects in magnetic fluid lubricated journal bearing, *Journal of Marine Science and Technology*, 24(4), p.p. 711-716.21 Patel, H. C., Deheri, G. M. and Patel, R. M., 2008, Performance of magnetic fluid based rotating rough circular step bearings, *International Journal of Applied Mechanics and Engineering*, 13(2), 441-455.

[23] Bhat, M., V. Bhat, Deheri, G. M. Deheri. 1993. Magnetic fluid-based squeeze film in curved porous circular disks, *Journal of Magnetism and Magnetic Material*, 127, 159-162.

